Received: 16 September 2025 | Accepted: 19 July 2026

DOI: 10.1111/2041-210x.70389

Methods in Ecology and Evolution

RESEARCH ARTICLE

Spatially realistic dynamic N-mixture models

Qing Zhao[1] | Paige E. Howell[2] | Erin Muths[3] | Brent H. Sigafus[4] | Blake R. Hossack[5,6] | Christopher E. Latimer[1]

[1]Bird Conservancy of the Rockies, Fort Collins, Colorado, USA; [2]National Raptor Program, Division of Migratory Bird Management, U.S. Fish and Wildlife Service, Washington, District of Columbia, USA; [3]Fort Collins Science Center, U.S. Geological Survey, Fort Collins, Colorado, USA; [4]Cooperative Fish and Wildlife Research Units, U.S. Geological Survey, University of Arizona, Tucson, Arizona, USA; [5]Northern Rocky Mountain Science Center, U.S. Geological Survey, Missoula, Montana, USA and [6]Wildlife Biology Program, W. A. Franke College of Forestry & Conservation, University of Montana, Missoula, Montana, USA

Correspondence
Qing Zhao
Email: qing.zhao@birdconservancy.org

Handling Editor: Chris Sutherland

Abstract

1. Dispersal is a complex ecological process that can be driven by the abiotic environment, density-dependent processes and species mobility. Traditionally, dispersal has been studied with capture-based data that are often limited in space and time. More recently, spatial dynamic N-mixture models (i.e. N-mixture models accounting for dispersal among local populations and changes in abundance over time) allow the study of dispersal with count data. However, current spatial dynamic N-mixture models focus mainly on distance-based dispersal, limiting our ability to evaluate realistic patterns and drivers of dispersal at relevant spatial and temporal scales.
2. We developed a spatially realistic dynamic N-mixture model that allows dispersal to be driven by environmental conditions and population density. Using simulations, we evaluated the inferential performance of this model when large proportions of sites are unsurveyed and the survey period is short, situations that are typical of real-world studies. We then used two case studies to illustrate the applications of this model, one representing a species with limited mobility in fragmented habitat (Chiricahua Leopard Frogs, *Lithobates chiricahuensis*, in isolated ponds) and the other representing a species with great mobility in continuous heterogeneous habitat (Common Nighthawks, *Chordeiles minor*, in grasslands).
3. Our simulation study showed that the model provides valid inference even when the number of surveyed sites is small ($n = 10$) or when the survey period is short for dynamic models (5 years), indicating that the model could have great practical value in real-world studies. The case study of Chiricahua Leopard Frogs showed that the model is capable of revealing pond-type-specific dispersal and predicting dispersal among ponds. The case study of Common Nighthawks showed the ability of the model to reveal the effect of primary productivity on dispersal and to map dispersal across the study area.

4. Our effort demonstrates the potential of using count data to gain insights about complex yet realistic dispersal processes. The model that we introduce is flexible and adaptable for a broad range of situations in population and conservation ecology.

KEYWORDS
count data, Dail–Madsen model, density dependence, dispersal movement, metapopulation, spatiotemporal statistics

1 | INTRODUCTION

Dispersal, the active or passive movement from a natal/breeding site to another breeding site, is a key ecological process that influences population distributions, dynamics and viability (Bowler & Benton, 2005; Cavanaugh et al., 2024; Clobert et al., 2001; Hanski, 1998). Because dispersal allows individuals to explore spatially and temporally varying resources, it is not necessarily random and can be influenced by environmental conditions (Clobert et al., 2009; Peniston et al., 2023; Swift et al., 2025). For instance, individuals may be more likely to leave low-quality habitats and settle in high-quality habitats (Fukuda et al., 2022; Haughland & Larsen, 2004; Lin & Batzli, 2001). Dispersal can also be influenced by density-dependent processes (Ims & Andreassen, 2005; Matthysen, 2005). Individuals may tend to leave sites with high local density or settle in sites with low local density to reduce intraspecific competition (De Bona et al., 2019) or leave high-quality habitats with low population density to avoid inbreeding (Szulkin & Sheldon, 2008; Wolff et al., 1988). Individuals may also be attracted by conspecific individuals during dispersal if social aggregations reduce their chance of being preyed on or provide cues for resource or mate availability (Korsten et al., 2013; Serrano & Tella, 2003).

Factors that influence dispersal also vary greatly across species, especially for species from distant taxonomic groups with different mobility (e.g. flight vs. foot) and ability to explore novel environments (Burgess et al., 2016). Species with limited mobility often lack knowledge of the surrounding environment, and thus, their dispersal is likely to be influenced by environmental conditions at source sites rather than destination sites (Pinto & MacDougall, 2010; Pittman et al., 2014; Shurin et al., 2009). By contrast, species with great mobility may be able to explore the surrounding environment thoroughly; thus, their dispersal may be influenced by environmental conditions at both source and destination sites, in accordance with the theory of ideal free distributions (Fretwell & Lucas, 1969; Haché et al., 2013; van der Hammen et al., 2012; Walhström & Kjellander, 1995; Zammarelli et al., 2024). Overall, dispersal is a complex ecological process that can be driven by the abiotic environment, density-dependent processes and species mobility.

Understanding the causes and consequences of dispersal is essential for predicting population responses to environmental alterations such as habitat fragmentation and climate change (Bailey & Muths, 2019; Doerr et al., 2011; Esler, 2000), but it is challenging to gain such understanding due to the above-mentioned complexity of dispersal. Furthermore, because dispersal is rarely observed directly, researchers have to rely on statistical models to infer such a process (e.g. Arnason, 1972, 1973; Howell et al., 2020; Zhao et al., 2017). Traditional metapopulation models (e.g. Hanski, 1994) and their modern counterparts, spatial dynamic occupancy models (e.g. Broms et al., 2016; Howell et al., 2018), have focused on explaining occurrence instead of the abundance of local populations. Consequently, while the colonization parameter estimated in these models may be related to dispersal, these models do not provide direct information about dispersal and its drivers. To explicitly allow dispersal in model structures, studies have relied on individual-based data (Arnason, 1972, 1973; Jønsson et al., 2016; Lebreton et al., 2009; McCrea et al., 2010; Schwarz et al., 1993; Zhao, 2020). However, these data are costly to collect and thus are often limited in space and time. Consequently, the small sample sizes of these data could limit the statistical power of the modelling approaches used to make population-wide inferences of dispersal (Hebblewhite & Haydon, 2010).

The original dynamic N-mixture model or Dail–Madsen model (Dail & Madsen, 2011) allows the estimation of two demographic parameters, apparent survival and recruitment, with counts of individuals in unmarked populations (Bellier et al., 2016; Madsen & Royle, 2023). Recent extensions of the dynamic N-mixture model explicitly represent dispersal in the model structure, allowing direct inference of dispersal with count data (Howell et al., 2020; Zhao et al., 2017). Due to the widespread nature of count data, these models can greatly improve our ability to study dispersal at the spatial and temporal scales relevant to this ecological process. However, so far, these models mainly focus on distance-based dispersal by assuming that dispersal probability between any pair of sites is determined by the Euclidean distance between these sites (Howell et al., 2020; Zhao et al., 2017). The potential of dynamic N-mixture models in accounting for more realistic dispersal patterns related to spatiotemporal variation in environmental conditions and population density remains to be investigated.

Another limitation of existing spatial models is that their performance when some sites are not surveyed has not been evaluated. Spatial models, unlike their non-spatial counterparts, require modelling every site in the study system because local populations from any site may influence other local populations through dispersal (e.g. Zhao, 2020, 2024). However, most surveys tend to cover only a portion of the sites in the study system due to time and financial

limitations. While abundance at these unsurveyed sites can be predicted through covariate relationships in spatial N-mixture models (e.g. Howell et al., 2020), the ability of these models to estimate dispersal when some sites are unsurveyed is unknown.

In this study, we developed a spatially realistic dynamic N-mixture model that allows for population dynamics to be influenced by local population growth and dispersal, both of which can be driven by environmental conditions and population density. We evaluated the inferential performance of this model with simulations while considering different proportions of unsurveyed sites and different lengths of the survey period. We then illustrated the applications of this model with two case studies in vastly different systems: the study of Chiricahua Leopard Frogs (*Lithobates chiricahuensis*) in isolated pond habitat represents a species with limited mobility in a fragmented habitat, and the study of Common Nighthawks (*Chordeiles minor*) in a grassland habitat represents a species with great mobility in a continuous yet heterogeneous habitat. Based on the results, we discussed the strengths and weaknesses of this model.

2 | METHODS

2.1 | Model description

The model contains a process sub-model that describes how site-level true abundance varies spatially and temporally, and an observation sub-model that describes how count data are obtained given true abundance. We assumed that our study system functioned as a metapopulation, with multiple habitat sites that could potentially be inhabited by local populations. We assumed that the metapopulation is isolated from other potential metapopulations of the study species and that the locations of all potential habitat sites in the area are known; consequently, we assumed that the metapopulation is closed from dispersal movement. In practice, it may be possible to identify all the insular habitats (e.g. ponds, forest remnants) in a study area and use them as habitat sites in the model. Alternatively, if the habitat is continuous, researchers could delineate the study area into a grid and use the grid cells as sites in the model. The closure assumption of the metapopulation can be relaxed when there are unidentified habitat sites within the study area, or when there are other metapopulations outside the study area that can have dispersal movement from/to the study metapopulation.

For local populations, we assumed that they are closed to mortality, reproduction and dispersal movement within each primary observation occasion (e.g. year) and allowed them to change between primary observation occasions. Furthermore, we assumed that the change in a local population is a consequence of local population growth at the corresponding site and dispersal among sites. When the metapopulation is closed, local population growth is due to true survival (i.e. individuals survive and *always* stay at one of the identified sites) and reproduction, and dispersal occurs only between identified sites. When the metapopulation is not closed, local population growth is due to apparent survival (i.e. individuals survive and stay at one of the identified sites) and reproduction, and dispersal can occur between identified and unidentified sites.

For the observation process, we assumed that each primary observation occasion can include multiple secondary observation occasions, that is, the robust sampling design (Kendall & Pollock, 1992; Pollock, 1982). Other sampling designs such as double observer (Nichols et al., 2000) or distance sampling (Royle et al., 2004) can be easily incorporated into this modelling framework to facilitate the estimation of the observation parameters.

2.1.1 | Process sub-model

We considered a system with I sites that are surveyed in T years. We assumed that the abundance of the study species at site i in year t, denoted $N_{i,t}$, follows a Poisson distribution such that $N_{i,t} \sim \text{Poisson}(\lambda_{i,t})$. For the first year (i.e. $t = 1$), we assumed that $\lambda_{i,1}$ is a function of K environmental covariates such that

$$\log(\lambda_{i,1}) = \beta_0^{[0]} + \sum_{k=1}^{K} \beta_k^{[0]} x_{k,i}, \tag{1}$$

with intercept and slope parameters $\beta^{[0]}$ representing the effects of environmental covariates on initial abundance.

For subsequent years (i.e. $t \geq 2$), we assumed that $\lambda_{i,t}$ is driven by both local population growth at any site j and dispersal from these sites to site i under the closure assumption of the metapopulation such that

$$\lambda_{i,t} = \sum_{j=1}^{I} \left(N_{j,t-1} \rho_{j,t} \theta_{j \to i,t}\right), \tag{2}$$

with local population growth rate $\rho_{j,t}$ and dispersal probability $\theta_{j \to i,t}$ (i.e. the probability of dispersing from site j to site i). When the closure assumption is relaxed, we can have $\lambda_{i,t} = \sum_{j=1}^{I} \left(N_{j,t-1} \rho_{j,t} \theta_{j \to i,t}\right) + \delta$, in which δ is the expected number of immigrants per site and year from unidentified sites (Hostetler & Chandler, 2015). Note that the effect of dispersal from identified sites to unidentified sites cannot be estimated separately and is accounted for in the local population growth rate $\rho_{j,t}$. Furthermore, we assumed that local population growth rate $\rho_{j,t}$ is driven by local population density and F environmental covariates and their interactions such that

$$\log(\rho_{j,t}) = \beta_0^{[\rho]} + \beta_D^{[\rho]} D_{j,t-1} + \sum_{f=1}^{F} \beta_f^{[\rho]} x_{f,j,t} + \sum_{f=1}^{F} \beta_{D \times f}^{[\rho]} D_{j,t-1} x_{f,j,t}, \tag{3}$$

with intercept and slope parameters $\beta^{[\rho]}$ representing the effects of density ($\beta_D^{[\rho]}$), environmental covariates ($\beta_f^{[\rho]}$) and their interactions ($\beta_{D \times f}^{[\rho]}$) on local population growth. Density $D_{j,t-1}$ is calculated as $N_{j,t-1} / A_j$, in which A_j is the area of site j. Note that the covariates here do not have to be the same as the covariates used in Equation (1).

In addition to local population growth, we also allowed individuals to disperse among local populations with an unnormalized dispersal probability $\eta_{j\to i,t}$, which is assumed to be a function of the Euclidean distance between sites, density and environmental covariates so that dispersal rate can vary both spatially and temporally:

$$\eta_{j\to i,t} = \exp\left(-\kappa d_{j,i} + \beta_D^{[\eta]} D_{j,i,t-1}^{[M]} + \sum_{h=1}^{H} \beta_h^{[\eta]} x_{h,j,i,t}^{[M]} + \sum_{h=1}^{H} \beta_{D\times h}^{[\eta]} D_{j,i,t-1}^{[M]} x_{h,j,i,t}^{[M]} \right), \quad (4)$$

with a dispersal rate parameter κ representing the effect of distance between sites j and i, $d_{j,i}$, as well as slope parameters $\beta^{[\eta]}$ representing the effects of density ($\beta_D^{[\eta]}$), H environmental covariates ($\beta_h^{[\eta]}$) and their interactions ($\beta_{D\times h}^{[\eta]}$) on dispersal. We then calculated a normalized dispersal probability $\theta_{j\to i,t} = \frac{\eta_{j\to i,t}}{\sum_{i=1}^{n_{\text{site}}} \eta_{j\to i,t}}$ so that the multinomial cell probabilities sum to 1 to be consistent with the fact that we only considered dispersal between identified sites in this equation. Note that dispersal from site j to site i includes the possibility of staying at site j, that is, when $j = i$ and $d_{j,i} = 0$. Consequently, a larger value of κ represents a lower probability of emigration (calculated as $1 - \theta_{j=i,t}$) and a shorter dispersal distance. We modelled dispersal as a function of the Euclidean distance among sites, while this distance metric could be replaced with others such as cost-weighted distance (Howell et al., 2018) or commute-time distance (Kervellec et al., 2024). In this study, we focused on improving the biological realism of the model by assuming that, even for the same distance, dispersal probability could be different because of the population density and environmental conditions at the source and destination sites. For example, the model allows dispersal from site j to site i to be influenced by the difference in density between two sites $D_{j,i,t}^{[M]}$ that could be calculated as $D_{j,i,t}^{[M]} = D_{i,t} - D_{j,t}$, and a negative $\beta_D^{[\eta]}$ means that individuals are less likely to move to site i if it has a higher density than site j and vice versa. The model also allows dispersal to be a function of environmental covariates $x_{h,j,i,t}^{[M]}$ that could be calculated as $x_{h,j,i,t}^{[M]} = x_{h,i,t} - x_{h,j,t}$, and a positive $\beta_h^{[\eta]}$ represents habitat selection for a higher $x_{h,i,t}$ value. Again, the covariates here do not have to be the same as the covariates in Equation (1).

While it is not required in the model structure, in practice, we scaled density in Equations (3 and 4) to facilitate convergence. More specifically, we had $D_{j,t}^{[\text{scaled}]} = \frac{D_{j,t} - \lambda_{j,1}/A_j}{\lambda_{j,1}/A_j}$ in Equation (3) so that the expected density in the first year was used as the baseline of density dependence in local population growth. We also had $D_{j,i,t}^{[M,\text{scaled}]} = \frac{D_{j,i,t}^{[M]}}{\exp(\beta_0^{[0]})}$ in Equation (4), so that the average expected density in the first year was used as the baseline of density dependence in dispersal.

2.1.2 | Observation sub-model

For the observation process, we considered multiple secondary observation occasions within each primary observation occasion under the robust sampling design (Kendall & Pollock, 1992; Pollock, 1982). We considered a binomial observation process such that $y_{i,t,l} \sim \text{Binomial}(N_{i,t}, p_{i,t,l})$, in which $y_{i,t,l}$ is the observed count during the lth secondary observation occasion at site i in year t, and the detection probability $p_{i,t,l}$ is a function of G observation covariates such that

$$\text{logit}(p_{i,t,l}) = \alpha_0 + \sum_{g=1}^{G} \alpha_g w_{g,i,t,l}, \quad (5)$$

with the intercept and slope parameters α representing the effects of observation covariates on detection probability.

2.1.3 | Data requirement

The model uses covariate data that can be organized into a covariate-by-site matrix for the initial abundance (Equation 1), a covariate-by-site-by-year array for local population growth (Equation 3) and a covariate-by-site-by-site-by-year array for dispersal movement (Equation 4). The model also needs a site-by-site distance matrix that can be calculated from site location information. The species data used in the model can be organized into a site-by-year-by-visit array for the robust sampling design and can be changed into other formats for different approaches such as double observer or distance sampling.

2.2 | Simulation study

We conducted three simulation studies to evaluate the inferential performance of the model. For these simulations, we simulated abundance at 100 sites during multiple years. Considering that most real-world studies could have ≥100 sites, this assumption should allow us to achieve a realistic understanding of model performance. The locations of sites were randomly drawn from a two-dimensional space such that $\text{easting} \sim \text{Uniform}(-10, 10)$ and $\text{northing} \sim \text{Uniform}(-8, 8)$, and all sites were assumed to have the same area. We first randomly drew values for a covariate representing landscape characteristics from a standard normal distribution such that $x_{i,t} \sim \text{Normal}(0, 1)$. For the first year, we assumed an average site-level abundance of about 6 ($\beta_0^{[0]} = 1.8$) and a positive effect of x on log abundance ($\beta_1^{[0]} = 1$). For the second year and beyond, we assumed that local population growth is driven by a negative effect of density, a positive effect of x as well as a positive interactive effect between density and x to represent a weaker negative density-dependent process in a better habitat on the log scale ($\beta_0^{[\rho]} = 0$, $\beta_D^{[\rho]} = -0.8$, $\beta_1^{[\rho]} = 0.6$, $\beta_{D\times 1}^{[\rho]} = 0.2$). We used a κ value of 2 to allow a moderate emigration probability and dispersal distance and assumed that dispersal rate is also driven by a negative effect of density, a positive effect of x as well as a positive interactive effect between density and x on the log scale ($\beta_D^{[\eta]} = -0.8$, $\beta_1^{[\eta]} = 0.6$, $\beta_{D\times 1}^{[\eta]} = 0.2$). We assumed that the metapopulation was closed for the first and second simulation studies and relaxed this assumption in the third simulation study.

In the first simulation study, we aimed to evaluate the performance of the model under different proportions of unsurveyed sites.

Therefore, we considered a fixed survey period of 20 years. We started with a scenario in which all sites were surveyed; while this scenario is unlikely to be achieved in real-world studies, we used it as a benchmark. We then considered a scenario with 50% unsurveyed sites (i.e. 50 surveyed sites) and a scenario with 90% unsurveyed sites (10 surveyed sites).

In the second simulation study, we aimed to evaluate the performance of the model under different study durations, when only some of the sites were surveyed. This time, we assumed that 67% of the sites were unsurveyed (33 surveyed sites). We then considered three scenarios representing survey periods of 20, 10 and 5 years, respectively.

In the third simulation study, we aimed to evaluate the performance of the model when the closure assumption of the metapopulation was relaxed. We considered a survey period of 20 years with 50% unsurveyed sites (i.e. 50 surveyed sites). We assumed that each site could have some immigrants from unidentified sites by having $\delta = 0.5$.

In all three simulation studies, we assumed a robust sampling design with multiple secondary observation occasions within each primary observation occasion. We considered a favourable observation situation with an average detection probability of 0.57 ($\alpha_0 = 0.3$) and five secondary observation occasions and a less favourable observation situation with an average detection probability of 0.29 ($\alpha_0 = -0.9$) and three secondary observation occasions. We randomly drew values for an observation covariate from a standard normal distribution such that $w_{i,t,l} \sim \text{Normal}(0, 1)$ and assumed that this covariate had a negative effect on detection probability on the logit scale ($\alpha_1 = -0.5$).

We simulated an environmental covariate in a site-by-year matrix and used it for initial abundance, local population growth and dispersal rate. We also simulated the distance between sites in a site-by-site matrix and used it for dispersal rate. We then simulated an observation covariate in a site-by-year-by-visit array and used it for detection probability. At last, we simulated count data in a site-by-year-by-visit array. When analysing the simulated data, we assigned missing values to the count data and observation covariates for unsurveyed sites, but we assumed that the locations and environmental covariates were available for all sites and used this information in the model.

We simulated 100 data sets for each scenario. We first calculated a coverage rate for each parameter as the proportion of simulations for which the 95% credible interval (CI) of the posterior samples covered the true value of the corresponding parameter. Furthermore, a Monte Carlo standard error could be calculated for the coverage rate as $\sqrt{0.95 \times (1 - 0.95) / 100} = 0.022$, leading to a 95% confidence interval of [0.91, 0.99] for the coverage rate (Morris et al., 2019). Therefore, we considered any coverage rate between 0.91 and 0.99 an indicator of valid inference of the model. We also calculated the average width of 95% CIs of the posterior samples across the 100 simulations as a measure of uncertainty such that $\overline{W} = \sum_{i=1}^{100} W_i / 100$, in which $\overline{W}$ is the average width and W_i is the width of the 95% CI of the posterior samples for the ith simulation. A higher $\overline{W}$ value indicated a higher uncertainty of the parameter estimates and vice versa. Note that $\overline{W}$ could be used to compare the inferential uncertainty of each parameter, but not among parameters.

2.3 | Case study 1: Chiricahua leopard frog

In the first case study, we considered a metapopulation of Chiricahua Leopard Frogs that inhabited artificial ponds in a semiarid grassland desert at Buenos Aires National Wildlife Refuge and the surrounding Altar Valley in southern Arizona (Howell et al., 2020). We used this system to represent the case of a species with limited mobility and knowledge about their surrounding landscape. We identified 274 ponds in the study area as potential sites and surveyed 44 (16.1%) of them in five consecutive years (2013–2017) during June, before the start of summer rains when the population was assumed to be closed (Howell et al., 2020). All possible breeding locations were identified using aerial photographs, topographic maps and ground searches. Distance between sites was calculated based on the centroid of each site. In each year, the surveyed sites were visited up to three times between 2100 h and 0300 h by two observers where frogs were counted visually. Therefore, the observation process represents a case with robust sampling design and a double observer framework (Nichols et al., 2000) to facilitate the estimation of detection probability. This research was conducted under AGFD Permits SP616031, SP674249 and SP713908; BANWR Special Use Permits 2013-013, 2017-008 and 2015-016; and USFWS Permit TE08548B; and IACUC 12-334 and A2014 01-028-Y2-A2. Animal ethics committee approval was not required because the researchers did not handle the animals for this study.

In the process sub-model, we considered a categorical environmental variable, pond type, as a potential predictor of local population growth and dispersal. Ponds were categorized as stable or temporary; while stable ponds generally hold water year-round or during the majority of a year, temporary ponds hold water less than half the year. This hydrological characteristic may influence population growth at ponds (Howell et al., 2020), but its effect on dispersal remains to be investigated. We used pond type as the only covariate for initial abundance (Equation 1) with an alternative parameterization that allows the intercept to differ between pond types, and thus have the intercepts $\beta^{[0]}_{\text{stable}}$ and $\beta^{[0]}_{\text{temporary}}$ for stable and temporary ponds, respectively. Similarly, we used the alternative parameterization to allow pond-type-specific intercept $\beta^{[\rho]}_{\text{intercept,stable}}$ and $\beta^{[\rho]}_{\text{intercept,temporary}}$ for local population growth (Equation 3). For dispersal, we modified the general model structure in Equation (4) to allow the dispersal rate parameter κ to differ between pond types and thus have κ_{stable} and $\kappa_{\text{temporary}}$. In addition to pond hydroperiod, we also allowed local population growth and dispersal to be influenced by a density-dependent process, represented by $\beta^{[\rho]}_{\text{density}}$ (Equation 3) and $\beta^{[\eta]}_{\text{density}}$ (Equation 4), respectively. We considered dispersal as a function of pond type and density at the source site but not the destination site because amphibians are considered to have limited

knowledge about their surrounding landscape (deMaynadier & Houlahan, 2007; Patrick et al., 2008; Pittman et al., 2014), and thus, their dispersal decision is unlikely to be based on habitat conditions at the destination. Because the metapopulation was isolated from other potential populations of the species, and all habitat sites in the metapopulation were identified by our field crew, we followed the closure assumption of the metapopulation for this case study.

In the observation sub-model, we used temperature and wind speed as two observation covariates for detection probability (Howell et al., 2020) with intercept and slope parameters $\alpha_{\text{intercept}}$, $\alpha_{\text{temperature}}$ and α_{wind} (Equation 5). To use the data in the model, the covariate pond type was organized into a vector with values for each site; pond area was also in a vector with values for each site; distance between ponds was in a site-by-site matrix; observation covariates were in two site-by-year-by-visit arrays (one for temperature and one for wind speed), and the count data were in two site-by-year-by-visit arrays (each for one observer).

The model provided parameter estimates that could be used to predict the dispersal probability of frogs between ponds. More specifically, we used the posterior median of κ_{stable} and $\kappa_{\text{temporary}}$ to predict the average dispersal probability between any pair of ponds i and j as $\left(\theta_{i\to j}+\theta_{j\to i}\right)/2$. We then plotted the predicted dispersal probability between any pair of sites in the study area.

2.4 | Case study 2: Common nighthawk

In the second case study, we considered a population of Common Nighthawks inhabiting grasslands in Kansas to represent the case of a species with great mobility in a continuous, yet heterogeneous, habitat. We divided the study area into 576 grid cells 20 km × 20 km in size that were considered sites in the model, which allowed for adequate habitat heterogeneity among sites that is meaningful to inform conservation practice. The locations of the centres of these grid cells were used to calculate the distances between sites. We used data from the Integrated Monitoring in Bird Conservation Regions (IMBCR) programme (Pavlacky et al., 2017) and data from the North American Breeding Bird Survey (BBS; Sauer et al., 2017) between 2011 and 2022 under a data integration framework (Zhao et al., 2024). The IMBCR programme adopts a probabilistic sampling design (Pavlacky et al., 2017; Stevens & Olsen, 2004) to allow unbiased representation of population abundance. The IMBCR programme also contains distance and removal sampling information and spatial replicates to facilitate estimation of observation errors. While BBS data may contain biases in representing local population size due to the vicinity of its routes to road, the widespread nature of its route allows us to achieve a better spatial coverage than using the IMBCR data alone. More specifically, in this way, 252 (43.8%) sites were covered by either IMBCR or BBS, with 142 (24.7%) covered by IMBCR but not BBS, 84 (14.6%) covered by BBS but not IMBCR, 26 (4.5%) covered by both and 324 (56.3%) not covered by either survey. All fieldwork of IMBCR was conducted under the appropriate federal, state and local permits, where required. Access to private lands was granted by the landowners with their free, prior and informed consent. No additional permissions were required. No birds were captured, handled, marked or otherwise disturbed, and the research did not involve any experimental manipulation. As a result, animal ethics committee approval was not required. No permit was needed to use BBS data as it is publicly available.

In the process sub-model, we considered Normalized Difference Vegetation Index (NDVI) summed over spring (March–May) derived from 250 m MODIS data (Didan, 2021) as the predictor of initial abundance ($\beta^{[0]}_{\text{NDVI}}$, Equation 1) and local population growth ($\beta^{[\rho]}_{\text{NDVI}}$, Equation 3) because this variable represents primary productivity that is important for insectivore birds (Bailey et al., 2004; Ng et al., 2022). In addition, we considered the effects of local density ($\beta^{[\rho]}_{\text{density}}$) and its interaction with spring sum NDVI ($\beta^{[\rho]}_{\text{density×NDVI}}$) on local population growth (Equation 3). For dispersal, in addition to the effect of distance (κ, Equation 4), we considered the difference in spring sum NDVI between the source site and the destination site as its predictor ($\beta^{[\eta]}_{\text{NDVI}}$, Equation 4) because of the great mobility of this species and its capability to explore potential breeding habitat during the late stage of spring migration (Renfrew et al., 2013). Because the metapopulation was unlikely to be isolated from other metapopulations of the species outside Kansas, we relaxed the closure assumption and estimated an immigration parameter from unidentified sites, δ.

In the observation sub-model, we linked both IMBCR and BBS data to the same underlying abundance, while different observation parameters were estimated for the two data sets, under a joint likelihood data integration framework (Zhao et al., 2024). For IMBCR data, we estimated the parameters for distance ($\sigma^{[\pi]}$) and removal sampling ($\theta^{[\pi]}$). For BBS data, we estimated a scaling parameter (χ_0) to correct potential biases contained in this data set (e.g. due to the fact that BBS was a roadside survey). We also considered variation across routes and observers as random effects with standard deviation parameters $\sigma^{[\chi]}_{\text{route}}$ and $\sigma^{[\chi]}_{\text{observer}}$, respectively, and the effect of being a new observer (a binary variable) as a fixed effect represented by $\tau^{[\chi]}$. Note that the approach of using IMBCR and BBS data here was different from Equation (5), and details can be found in Zhao et al. (2024). To use the data in the model, we organized the covariate NDVI data into a site-by-year matrix and distance between sites into a site-by-site matrix. IMBCR counts were organized into a matrix with each row representing a combination of site and year, and each column representing a combination of distance bin and time interval. BBS counts were organized into a matrix with each row representing a combination of route and observer and each column representing a stop.

We used the posterior median of κ and $\beta^{[\eta]}_{\text{NDVI}}$ to predict the dispersal probability $\theta_{i\to j,t}$ between any pair of sites i and j in year t. We then calculated net dispersal probability as the difference between immigration $\sum_{j\neq i}\theta_{j\to i,t}$ and emigration $1-\theta_{i=j,t}$ for any site i in year t. This allowed us to visualize the spatial and temporal variation of net dispersal in the study area.

2.5 | Model implementation

We conducted Markov chain Monte Carlo (MCMC) computing in Nimble (de Valpine et al., 2017) through the R programming language (R Development Core Team, 2019). The No U-Turn Sampler (NUTS) was used via the nimbleHMC package (Turek et al., 2025). We used a vague prior $Normal(\text{mean} = 0, \text{SD} = 2)$ for $\beta^{[0]}$, $\beta^{[\rho]}$, $log(\kappa)$, $\beta^{[\eta]}$, $log(\delta)$ and α. For case study 2, we also used a vague prior $\text{Normal}(\text{mean} = 0, \text{SD} = 2)$ for $\log(\sigma^{[\pi]})$, $\text{logit}(\theta^{[\pi]})$, $\log(\chi_0)$, $\log\left(\sigma^{[\chi]}_{\text{route}}\right)$, $\log\left(\sigma^{[\chi]}_{\text{observer}}\right)$ and $\tau^{[\chi]}$ in the observation sub-model.

To generate posterior samples, we used three chains and 2000 iterations including 1000 burn-in without thinning for the simulation study, and three chains and 10,000 iterations including 8000 burn-in without thinning for the case studies. The convergence of the MCMC computing was checked using the diagnostic plot of the posterior samples and Brooks–Gelman–Rubin diagnostics, where $\hat{R} \leq 1.05$ was considered indicative of convergence for both simulation and case studies (Brooks & Gelman, 1998). For both case studies, we reported the median and 95% credible interval of the parameter estimates. For slope parameters, we also reported a posterior probability of direction (PD) statistic to represent the certainty of the parameter estimates. The PD statistic was calculated as the proportion of the posterior samples that were in the same direction as the posterior median and thus would always be greater than or equal to 0.5. We then considered the effect of a covariate supported when PD was >0.9, uncertain when PD was 0.60–0.90 and no effect when PD was <0.6.

3 | RESULTS

3.1 | Simulation study

We considered combinations of different proportions of surveyed sites, survey periods and both a favourable and a less favourable observation situation in our simulations. The results showed that coverage values were between 0.91 and 0.99 under any scenario we considered, indicating that our model provided valid inference under the closure assumption of metapopulation (Tables 1 and 2) or when the assumption was relaxed (Table 3). The uncertainty of the parameter estimates, represented by the average width of the 95% CIs of posterior samples, increased as the proportion of unsurveyed sites increased (Table 1) or when the study period decreased (Table 2). The uncertainty of the parameter estimates was also higher under the less favourable observation situation than under the favourable observation situation (Tables 1 and 2). Nonetheless, the model provided valid inference even when only 10 out of 100 sites were surveyed for a 20-year study, or when 33 out of 100 sites were surveyed for a 5-year study, suggesting that this model is highly applicable in real-world studies.

TABLE 1 Coverage rate as an evaluation of model validity and average width of 95% credible intervals of posterior samples as a measure of model uncertainty during a survey period of 20 years when 100%, 50% or 10% of 100 sites are surveyed.

Parameter	True value	Coverage						Width of CI					
Observation conditions		High detection, 5 secondary observation occasions			Low detection, 3 secondary observation occasions			High detection, 5 secondary observation occasions			Low detection, 3 secondary observation occasions		
Proportion of surveyed sites		100%	50%	10%	100%	50%	10%	100%	50%	10%	100%	50%	10%
$\beta^{[0]}_{\text{intercept}}$	1.8	0.96	0.94	0.96	0.94	0.91	0.95	0.16	0.22	0.43	0.23	0.31	0.58
$\beta^{[0]}_{\text{environment}}$	1	0.96	0.94	0.95	0.95	0.95	0.91	0.08	0.11	0.25	0.09	0.13	0.32
$\beta^{[\rho]}_{\text{intercept}}$	0	0.95	0.95	0.93	0.92	0.95	0.94	0.12	0.17	0.36	0.15	0.20	0.43
$\beta^{[\rho]}_{\text{density}}$	−0.8	0.93	0.96	0.95	0.94	0.94	0.96	0.16	0.22	0.50	0.20	0.28	0.67
$\beta^{[\rho]}_{\text{environment}}$	0.6	0.94	0.96	0.92	0.95	0.92	0.92	0.06	0.09	0.20	0.07	0.11	0.26
$\beta^{[\rho]}_{\text{density×environment}}$	0.2	0.94	0.95	0.93	0.95	0.95	0.96	0.08	0.11	0.26	0.09	0.14	0.40
κ	2	0.93	0.95	0.94	0.93	0.96	0.95	0.16	0.23	0.54	0.21	0.29	0.78
$\beta^{[\eta]}_{\text{density}}$	−0.8	0.95	0.94	0.95	0.95	0.94	0.93	0.15	0.21	0.47	0.19	0.26	0.62
$\beta^{[\eta]}_{\text{environment}}$	0.6	0.95	0.94	0.95	0.95	0.94	0.95	0.10	0.16	0.40	0.14	0.20	0.50
$\beta^{[\eta]}_{\text{density×environment}}$	0.2	0.95	0.95	0.94	0.95	0.94	0.93	0.06	0.09	0.23	0.07	0.10	0.29
$\alpha_{\text{intercept}}$	0.3	0.94	0.94	0.94				0.09	0.13	0.28			
	−0.9				0.93	0.92	0.91				0.21	0.29	0.53
α_{slope}	−0.5	0.94	0.94	0.94	0.95	0.92	0.93	0.04	0.06	0.13	0.06	0.09	0.19

TABLE 2 Coverage rate as an evaluation of model validity and average width of 95% credible intervals of posterior samples as a measure of model uncertainty when 33% of 100 sites are surveyed during a survey period of 20, 10 or 5 years.

Parameter	True value	Coverage						Width of CI					
Observation conditions		High detection, 5 secondary observation occasions			Low detection, 3 secondary observation occasions			High detection, 5 secondary observation occasions			Low detection, 3 secondary observation occasions		
Survey period (years)		20	10	5	20	10	5	20	10	5	20	10	5
$\beta^{[0]}_{\text{intercept}}$	1.8	0.96	0.95	0.95	0.95	0.93	0.95	0.27	0.28	0.30	0.38	0.45	0.60
$\beta^{[0]}_{\text{environment}}$	1	0.94	0.94	0.96	0.95	0.95	0.95	0.14	0.16	0.19	0.18	0.21	0.24
$\beta^{[\rho]}_{\text{intercept}}$	0	0.96	0.96	0.92	0.94	0.94	0.94	0.21	0.22	0.27	0.26	0.29	0.35
$\beta^{[\rho]}_{\text{density}}$	−0.8	0.96	0.95	0.94	0.93	0.92	0.96	0.28	0.34	0.50	0.35	0.45	0.67
$\beta^{[\rho]}_{\text{environment}}$	0.6	0.95	0.96	0.93	0.93	0.95	0.95	0.11	0.15	0.21	0.14	0.19	0.29
$\beta^{[\rho]}_{\text{density×environment}}$	0.2	0.95	0.96	0.94	0.94	0.94	0.95	0.14	0.21	0.36	0.18	0.27	0.46
κ	2	0.95	0.95	0.92	0.96	0.94	0.95	0.29	0.40	0.62	0.37	0.58	0.86
$\beta^{[\eta]}_{\text{density}}$	−0.8	0.95	0.94	0.95	0.95	0.95	0.95	0.26	0.31	0.41	0.33	0.41	0.56
$\beta^{[\eta]}_{\text{environment}}$	0.6	0.96	0.93	0.94	0.96	0.96	0.92	0.19	0.27	0.43	0.26	0.37	0.56
$\beta^{[\eta]}_{\text{density×environment}}$	0.2	0.96	0.94	0.94	0.93	0.95	0.93	0.11	0.14	0.19	0.14	0.18	0.28
$\alpha_{\text{intercept}}$	0.3	0.94	0.94	0.93				0.16	0.22	0.31			
	−0.9				0.91	0.93	0.95				0.34	0.48	0.74
α_{slope}	−0.5	0.93	0.95	0.93	0.95	0.93	0.94	0.07	0.10	0.14	0.11	0.15	0.21

TABLE 3 Coverage rate as an evaluation of model validity and average width of 95% credible intervals of posterior samples as a measure of model uncertainty when the closure assumption of the metapopulation is relaxed.

Parameter	True value	Coverage		Width of CI	
Observation conditions		High detection, 5 secondary observation occasions	Low detection, 3 secondary observation occasions	High detection, 5 secondary observation occasions	Low detection, 3 secondary observation occasions
$\beta^{[0]}_{\text{intercept}}$	1.8	0.96	0.91	0.22	0.29
$\beta^{[0]}_{\text{environment}}$	1	0.95	0.93	0.12	0.13
$\beta^{[\rho]}_{\text{intercept}}$	0	0.95	0.95	0.19	0.22
$\beta^{[\rho]}_{\text{density}}$	−0.8	0.94	0.95	0.23	0.29
$\beta^{[\rho]}_{\text{environment}}$	0.6	0.96	0.96	0.09	0.11
$\beta^{[\rho]}_{\text{density×environment}}$	0.2	0.96	0.94	0.11	0.15
κ	2	0.94	0.93	0.30	0.34
$\beta^{[\eta]}_{\text{density}}$	−0.8	0.95	0.93	0.24	0.27
$\beta^{[\eta]}_{\text{environment}}$	0.6	0.94	0.94	0.18	0.22
$\beta^{[\eta]}_{\text{density×environment}}$	0.2	0.94	0.94	0.09	0.11
δ	0.5	0.94	0.92	0.46	0.48
$\alpha_{\text{intercept}}$	0.3	0.92		0.12	
	−0.9		0.91		0.28
α_{slope}	−0.5	0.93	0.92	0.06	0.08

3.2 | Case study 1: Chiricahua leopard frog

We found that pond type influenced initial abundance, local population growth and dispersal of Chiricahua Leopard Frogs. More specifically, stable ponds had a higher abundance (median 19.30, 95% CI [16.91, 22.05]) than temporary ponds (0.23 [0.09, 0.45]), and populations in stable ponds had a higher local population growth rate (1.68 [1.59, 1.78]) than the populations in temporary ponds (0.89 [0.67, 1.15]; Table 4; Figure 1). Frogs in stable ponds were less likely to emigrate (κ_{stable} 156.52 [80.95, 1131.27]), and when they did, they tended to move a shorter distance than frogs from temporary ponds ($\kappa_{\text{temporary}}$ 8.64 [2.30, 177.17] with the unit of distance being 1 km; Table 4). Consequently, on average, there would be a 39.2% probability of individuals dispersing 0.1 km or more from a temporary pond, compared to a 0.0% probability of dispersing from stable ponds at the same distance (Figure 1). Our results supported a negative effect of density dependence on the local population growth of these frogs (−0.03 [−0.04, −0.03], PD = 1.000), but not on their dispersal (0.19 [−3.76, 4/19], PD = 0.533; Table 4; Figure 1). The model estimated an average detection probability of 0.36 [0.35, 0.38] which was positively influenced by temperature (0.38 [0.31, 0.46]) and wind speed (0.29 [0.24, 0.34]; Table 4). The model also allowed us to predict and visualize average dispersal probability between any pair of sites; frogs sometimes did not disperse between stable ponds directly but instead used temporary ponds as stepping stones (Figure 2).

TABLE 4 Parameter estimates (posterior medians and 95% credible intervals [CI]) for the case study of Chiricahua Leopard Frogs. A posterior probability of direction (PD) statistic is also reported for slope parameters.

Parameter	Median	95% CI	PD
Initial abundance			
Stable pond $\exp\left(\beta^{[0]}_{\text{stable}}\right)$	19.30	[16.91, 22.05]	
Temporary pond $\exp\left(\beta^{[0]}_{\text{temporary}}\right)$	0.23	[0.09, 0.45]	
Mean population growth			
Stable pond $\exp\left(\beta^{[\rho]}_{\text{intercept,stable}}\right)$	1.68	[1.59, 1.78]	
Temporary pond $\exp\left(\beta^{[\rho]}_{\text{intercept,temporary}}\right)$	0.89	[0.67, 1.15]	
Density dependence on population growth $\beta^{[\rho]}_{\text{density}}$	−0.03	[−0.04, −0.03]	1.000
Distance effect on dispersal			
Stable pond κ_{stable}	156.52	[80.95, 1131.27]	
Temporary pond $\kappa_{\text{temporary}}$	8.64	[2.30, 177.17]	
Density dependence on dispersal $\beta^{[\eta]}_{\text{density}}$	0.19	[−3.76, 4.19]	0.533
Detection			
Mean $\text{logit}^{-1}(\alpha_{\text{intercept}})$	0.36	[0.35, 0.38]	
Temperature effect $\alpha_{\text{temperature}}$	0.38	[0.31, 0.46]	1.000
Wind speed effect α_{wind}	0.29	[0.24, 0.34]	1.000

3.3 | Case study 2: Common nighthawk

We found that spring sum NDVI had supported positive effects on the initial abundance (0.21 [0.03, 0.36], PD = 0.991) and local population growth (0.11 [0.04, 0.22], PD = 1.000; Table 5) of Common Nighthawks in Kansas. Spring sum NDVI also had a positive but uncertain effect on the dispersal of the birds (0.21 [−0.45, 0.77], PD = 0.749; Table 5). Furthermore, there was a supported negative effect of density-dependent processes (−0.05 [−0.12, 0.01], PD = 0.943) with a supported negative interactive effect of local density and spring sum NDVI (−0.29 [−0.49, −0.16], PD = 1.000; Table 5) on local population growth, indicating that the positive effect of spring sum NDVI on local population growth was stronger when local density was lower (Figure 3). The small estimates of κ (1.25 [1.08, 1.50] with the unit of distance being 10 km; Table 5) meant that the birds could disperse for a long distance (e.g. >30 km; Figure 3). The model estimated a small number of immigrants per site and year from unidentified sites δ (0.08 [0.01, 0.31]; Table 5). The model also estimated a number of detection-related parameters for the IMBCR and BBS data (Table 5). Using the parameter estimates obtained from the model, we predicted a spatial gradient of net dispersal probability, with western and central Kansas having a higher probability of emigration than immigration, and eastern Kansas having a higher probability of immigration than emigration (Figure 4). The predicted net dispersal also showed evidence of temporal variation, for example, the area with a higher probability of immigration than emigration was about one-third of Kansas from 2011 to 2012 but shrank to the easternmost part of Kansas from 2020 to 2021 (Figure 4).

4 | DISCUSSION

We developed a spatially realistic dynamic N-mixture model that allows dispersal to be driven by environmental and density covariates. We then used simulations to show that the model can provide valid inference even when a small proportion of sites are surveyed and when the survey period is short, indicating that the model has great practical value in real-world studies. Using two case studies, we showed that the model can be used to evaluate drivers of dispersal and predict range-wide dispersal patterns. Because N-mixture models require only count data that are often available at broad spatial and temporal scales, we expect this model to be useful to provide inference of dispersal at the population level in a broad range of systems.

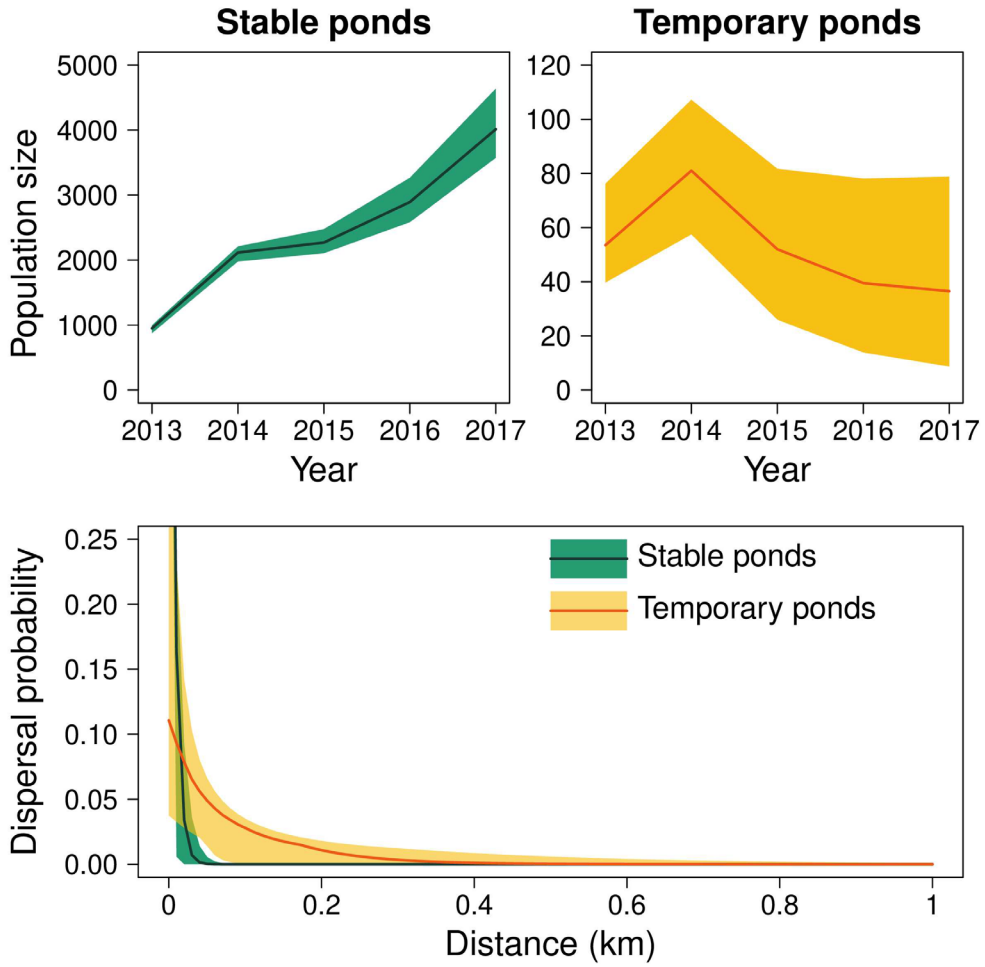

FIGURE 1 Estimated total population size of Chiricahua Leopard Frogs in stable ponds (top left panel) and temporary ponds (top right panel) from 2013 to 2017, and the response curve representing the relationship between dispersal probability and distance for frogs originating at stable or temporary ponds (lower panel). Total population size was calculated as the sum of the pond-level abundance for all the ponds in each pond type. Note that the probability at distance 0 (i.e. the left end of the curve) represents the probability of staying at the original pond (i.e. $\theta_{j=i}$) and the probability of emigration is calculated as $1-\theta_{j=i}$.

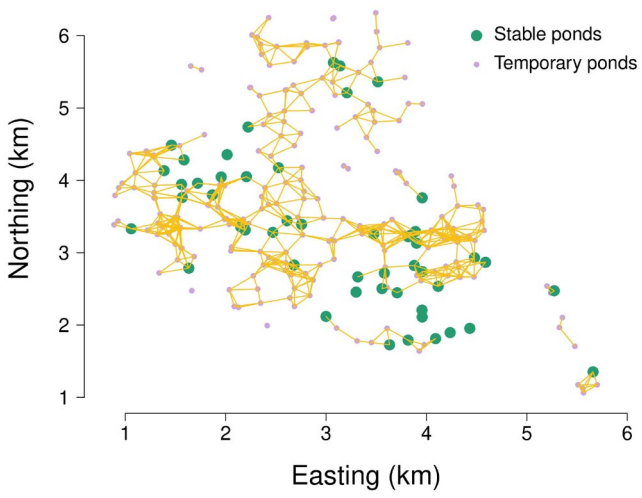

FIGURE 2 Predicted average dispersal probability ($\frac{\theta_{i\to j}+\theta_{j\to i}}{2}>0$ represented by yellow line segments) of Chiricahua Leopard Frogs in the study area. The frogs were predicted to sometimes disperse between stable ponds through temporary ponds.

4.1 | Model performance

The inferential performance of spatial dynamic N-mixture models has thus far been evaluated without considering missing values due to unsurveyed sites (Howell et al., 2020; Zhao et al., 2017, 2022). However, we argue that it is important to model both surveyed and unsurveyed sites in spatial models because all sites may influence each other through dispersal. It is encouraging that, in our simulation study, the spatially realistic dynamic N-mixture model can provide valid inference for all parameters, including those related to dispersal, even when only 10% of the sites are surveyed. Simulations also showed that our model provides unbiased parameter estimates when the survey period is as short as 5 years and 33% of the sites are surveyed. Because it is challenging to cover a large proportion of sites or conduct long-term surveys in real-world studies, our simulations demonstrate the practical value of the model introduced in this study. In our simulations, we considered a small total number of sites (100), which is often achievable in real-world studies. Furthermore, we considered a reasonable level of average abundance (6) and a low

TABLE 5 Parameter estimates (posterior medians and 95% credible intervals [CI]) for the case study of Common Nighthawks. A posterior probability of direction (PD) statistic is also reported for slope parameters.

Parameter	Median	95% CI	PD
Initial abundance			
Mean $\exp\left(\beta_0^{[0]}\right)$	3.74	[2.99, 4.61]	
NDVI effect $\beta_{\text{NDVI}}^{[0]}$	0.21	[0.03, 0.36]	0.991
Population growth			
Mean $\exp\left(\beta_0^{[\rho]}\right)$	0.97	[0.90, 1.03]	
Density dependence $\beta_{\text{density}}^{[\rho]}$	−0.05	[−0.12, 0.01]	0.943
NDVI effect $\beta_{\text{NDVI}}^{[\rho]}$	0.11	[0.04, 0.22]	1.000
Density × NDVI $\beta_{\text{density×NDVI}}^{[\rho]}$	−0.29	[−0.49, −0.16]	1.000
Dispersal			
Distance effect κ	1.25	[1.08, 1.50]	
NDVI effect $\beta_{\text{NDVI}}^{[\eta]}$	0.21	[−0.45, 0.77]	0.749
Immigration from unidentified sites δ	0.08	[0.01, 0.31]	
IMBCR detection			
Distance sampling $\sigma^{[\pi]}$	62.05	[56.57, 68.81]	
Removal sampling $\theta^{[\pi]}$	0.45	[0.40, 0.51]	
BBS detection			
Scaling parameter χ_0	0.04	[0.03, 0.06]	
Standard deviation of route variation $\sigma_{\text{route}}^{[\chi]}$	0.86	[0.60, 1.18]	
Standard deviation of observer variation $\sigma_{\text{observer}}^{[\chi]}$	1.04	[0.79, 1.42]	
New observer effect $\tau^{[\chi]}$	−0.71	[−1.16, −0.34]	1.000

average detection probability (0.30) in our simulations. Since studies have found that spatial dynamic N-mixture models could perform well under a lower abundance level and detection probability (Zhao et al., 2017; Zhao & Royle, 2019), we believe that the model introduced in the current study could perform as well, if not better, in real-world studies than in our simulations. We also extended the model to allow immigration from unidentified sites, which again provides valid inference and thus broadens the utility of this model. Further studies could consider modelling immigration from unidentified sites as a function of relevant covariates.

4.2 | Real-world applications

Using real-world data, we further showed that our model is flexible and adaptable to provide insights about complex ecological processes in vastly different systems, one representing a species with limited mobility in a fragmented habitat and the other representing a species with great mobility in a continuous yet heterogeneous habitat. The case studies also illustrated the flexibility of our model in incorporating data collected under different approaches such as double-observer visual survey, distance sampling and data integration.

For the Chiricahua Leopard Frog case study, our results showed that stable ponds had higher population density and local population growth rate than temporary ponds, indicating that the former is likely to be a better habitat than the latter (Howell et al., 2020). The negative density dependence on local population growth found in our study area likely reflects crowding and resource limitation under high local population densities (Patrick et al., 2008; Wells, 1977). We did not detect an effect of density on dispersal; although somewhat counterintuitive, frogs are able to tolerate extremely high local density (Patrick et al., 2008) without necessarily responding to it behaviourally (i.e. leaving). Overall, little is known about the drivers of dispersal in Chiricahua Leopard Frogs and amphibians in general (deMaynadier & Houlahan, 2007; Pittman et al., 2014).

Our model provides knowledge about pond-type-specific dispersal for Chiricahua Leopard Frogs that may also be relevant to other pond-dwelling amphibians. More specifically, our results showed that the frogs are more likely to stay in presumably more favourable stable ponds and are more likely to leave the less favourable temporary ponds. In addition, when they leave temporary ponds, they tend to move a longer distance than when they leave stable ponds, suggesting stronger exploration efforts by dispersers from poorer habitats (Haughland & Larsen, 2004).

Our model also predicted that frogs may disperse between stable ponds through temporary ponds, likely due to the longer dispersal distance from temporary ponds (Figure 2). While previous studies have pointed out the importance of maintaining and creating stable ponds for the conservation of this species (Howell et al., 2020), which our study echoes, our results further indicate the importance of temporary ponds in maintaining the integrity of the habitat for a metapopulation. Even though temporary ponds only harbour a small proportion of the entire population, increasing the number of temporary ponds may facilitate gene flow (i.e. provide stepping stones) among stable ponds and improve the persistence of the metapopulation in the face of environmental changes (Bailey & Muths, 2019; Campbell Grant et al., 2010). Overall, our model could be used to identify the importance of both high quality (e.g. source) and low quality (e.g. sink) habitat by considering habitat-related dispersal (Foppen et al., 2000; Howe et al., 1991), and thus provide new insights into the conservation of metapopulations.

For the Common Nighthawk case study, we found that spring sum NDVI, which represents cumulative vegetation productivity over the spring (April to June) when birds are setting up breeding territories,

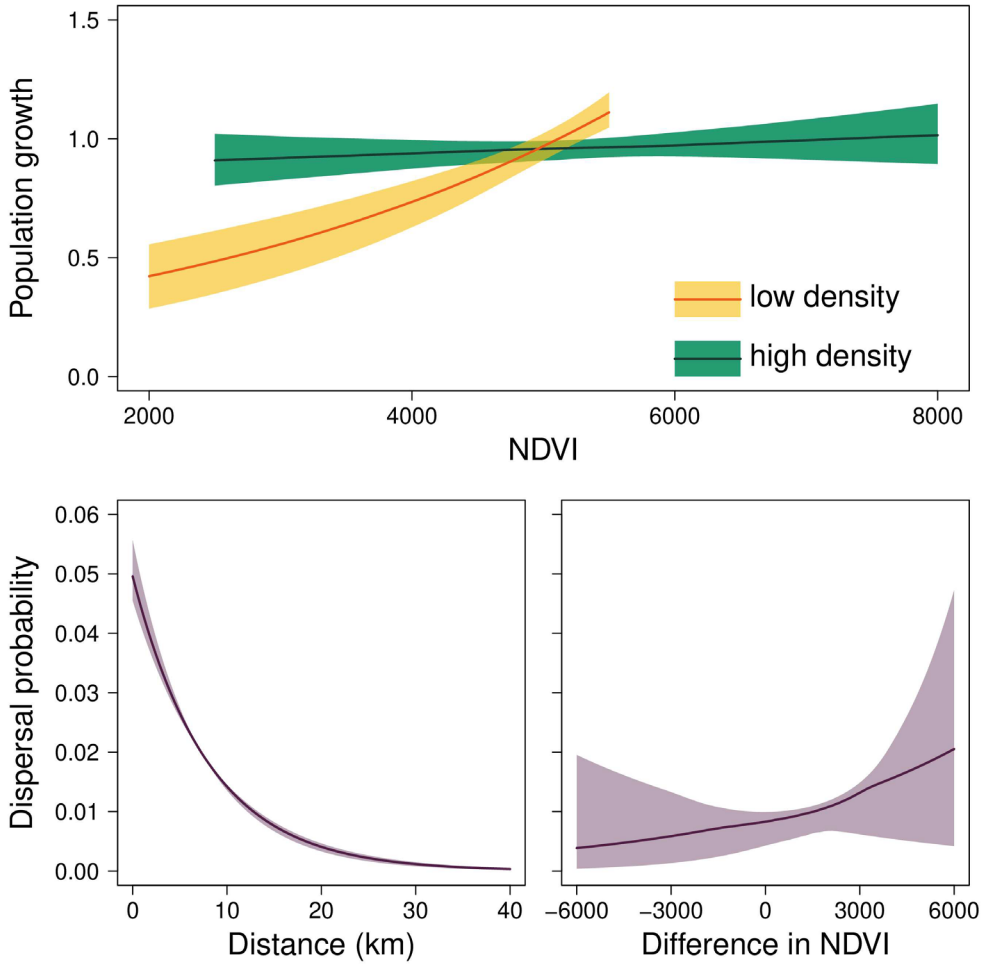

FIGURE 3 Response curves representing the effect of spring sum NDVI on local population growth under low and high local density (upper panel), the effect of distance on dispersal (lower left panel), and the effect of the difference in spring sum NDVI between the source and destination sites on dispersal of Common Nighthawks (lower right panel).

positively influenced their distribution, local population growth and dispersal. This finding supports the prediction that primary productivity plays a key role in shaping the distribution and population dynamics of this avian insectivore. Previous studies have linked bird abundance and movement to primary productivity which serves as a strong indicator of the food resources required to support their high energy demands (Bailey et al., 2004; Ng et al., 2022; Renfrew et al., 2013). We also found that local population density and spring sum NDVI interactively influenced local population growth. More specifically, local populations with high densities seemed to remain stable regardless of the variation of primary productivity, while local populations with low densities were strongly influenced by primary productivity. These results indicate that individuals inhabiting areas with high primary productivity are likely to form the core, stable portion of the population, while individuals inhabiting areas with low primary productivity seem to represent a less stable portion of the population.

Furthermore, our results also showed that this species is capable of long-distance dispersal, like other highly mobile species (Haché et al., 2013). Such long-distance dispersal allows them to move from unsuitable to suitable habitat, potentially revealing their ability to explore the environment at a broad spatial scale and select high-quality habitats based on available resources (Fretwell & Lucas, 1969; Zammarelli et al., 2024). Since the birds tend to move into areas with high primary productivity that can sustain the local populations, this pattern of resource-driven dispersal may represent an adaptive strategy for the species. Thus, our results indicate that areas with high primary productivity are important for the conservation of this and potentially other insectivorous bird species. Overall, our model provides a comprehensive view of dispersal, local population growth and spatiotemporal variation in abundance, making it a valuable tool for identifying areas of high conservation value.

4.3 | Future development

One constraint of our model is that both the probability of emigration and the distance of dispersal are related to the same parameter, κ. More specifically, a large value of κ leads to both a low probability of emigration and a short dispersal distance and vice versa. This

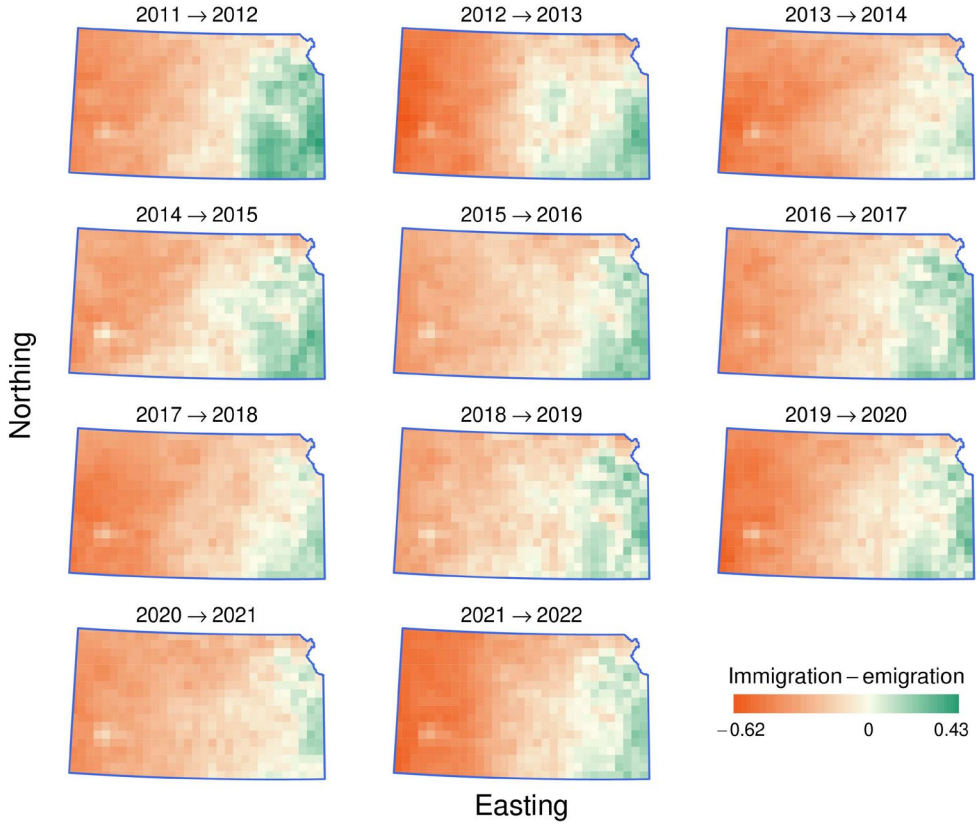

FIGURE 4 Predicted net dispersal (immigration–emigration) of Common Nighthawks in the Kansas grassland ecosystem. The figure shows the predicted spatial gradient and temporal variation of net dispersal. Green colours indicate areas that gained individuals (a higher probability of immigration than emigration) and orange colours indicate areas that lost individuals (a higher probability of emigration than immigration).

means the model does not allow situations where a small proportion of individuals emigrate but tend to disperse far, or a large proportion of individuals emigrate but tend to immigrate into adjacent areas. Some preliminary analyses lead us to believe it is necessary to combine capture–recapture data with count data to release the above-mentioned constraint (Zhao, 2020). Indeed, the model introduced in the current study can be used as a sub-model in integrated population models (Besbeas et al., 2002; Brooks et al., 2004; Schaub & Abadi, 2011; Schaub & Kéry, 2022), which could also allow us to separate the effect of survival and reproduction on local population growth and thus estimate the entire BIDE (i.e. birth, immigration, death, emigration) process.

Using a case study of the Common Nighthawks, we illustrated the potential of integrating multiple sets of count data with different qualities and spatiotemporal coverages in our model. The flexible structure of the model makes it possible to incorporate other types of unmarked data such as autonomously recorded data (Clement et al., 2022) and/or consider non-linear relationships (Leirs et al., 1997) under a framework of integrated distribution models (Fletcher et al., 2019; Miller et al., 2019; Pacifici et al., 2017; Zhao et al., 2024). Integrating multiple sets of count data and capture–recapture data is also a future direction for this class of models (Van Ee et al., 2024). Overall, data integration can allow for estimating additional parameters, achieving improved precision and/or extending the spatiotemporal coverage of the inference (e.g. Pacifici et al., 2017; Schaub & Abadi, 2011; Zhao, 2020; Zhao et al., 2024), and thus could be considered for the modelling framework introduced in the current study.

5 | CONCLUSION

We developed a spatially realistic dynamic N-mixture model for the inference of complex dispersal patterns at the population level with count data only. Using both simulated and real-world data, we showed that the model is reliable and capable of providing important insights and predictions about dispersal and population distributions and dynamics, which is challenging to achieve with individual-based data. Thus, we believe that this model is highly relevant to population ecology and conservation ecology.

AUTHOR CONTRIBUTIONS

Qing Zhao conceived the idea, conducted the analysis and wrote the manuscript. Paige Howell, Erin Muths, Brent Sigafus and Blake Hossack guided the development of the model for the frog case study and helped interpret the results. Chris Latimer guided the

development of the model for the bird case study and helped interpret the results. All co-authors provided critical reviews of the manuscript.

ACKNOWLEDGEMENTS

We thank C. Labuzzetta and E. Zylstra for helpful comments on an earlier draft of this manuscript. We thank three reviewers for helpful comments on the manuscript. Any use of trade, firm or product names is for descriptive purposes only and does not imply endorsement by the U.S. Government. This is contribution number 954 of the U.S. Geological Survey Amphibian Research and Monitoring Initiative (ARMI).

FUNDING INFORMATION

None.

CONFLICT OF INTEREST STATEMENT

The authors have no conflict of interest to declare.

PEER REVIEW

The peer review history for this article is available at https://www.webofscience.com/api/gateway/wos/peer-review/10.1111/2041-210x.70389.

DATA AVAILABILITY STATEMENT

The data and code used in this study are available via https://doi.org/10.5281/zenodo.21535376 (Zhao, 2026).

ORCID

Qing Zhao https://orcid.org/0000-0003-2759-1114

Blake R. Hossack https://orcid.org/0000-0001-7456-9564

REFERENCES

Arnason, A. N. (1972). Parameter estimates from mark-recapture experiments on two populations subject to migration and death. *Researches on Population Ecology*, *13*, 97–113.

Arnason, A. N. (1973). The estimation of population size, migration rates and survival in a stratified population. *Researches on Population Ecology*, *15*, 1.

Bailey, L. L., & Muths, E. (2019). Integrating amphibian movement studies across scales better informs conservation decisions. *Biological Conservation*, *236*, 261–268.

Bailey, S. A., Horner-Devine, M. C., Luck, G., Moore, L. A., Carney, K. M., Anderson, S., Betrus, C., & Fleishman, E. (2004). Primary productivity and species richness: Relationships among functional guilds, residency groups and vagility classes at multiple spatial scales. *Ecography*, *27*, 207–217.

Bellier, E., Kéry, M., & Schaub, M. (2016). Simulation-based assessment of dynamic N-mixture models in the presence of density dependence and environmental stochasticity. *Methods in Ecology and Evolution*, *7*, 1029–1040.

Besbeas, P., Freeman, S. N., Morgan, B. J. T., & Catchpole, E. A. (2002). Integrating mark-recapture-recovery and census data to estimate animal abundance and demographic parameters. *Biometrics*, *58*, 540–547.

Bowler, D. E., & Benton, T. G. (2005). Causes and consequences of animal dispersal strategies: Relating individual behaviour to spatial dynamics. *Biological Reviews*, *80*, 205–225.

Broms, K. M., Hooten, M. B., Johnson, D. S., Altwegg, R., & Conquest, L. L. (2016). Dynamic occupancy models for explicit colonization processes. *Ecology*, *97*, 194–204.

Brooks, S. P., & Gelman, A. (1998). General methods for monitoring convergence of iterative simulations. *Journal of Computational and Graphical Statistics*, *7*, 434–455.

Brooks, S. P., King, R., & Morgan, B. J. T. (2004). A Bayesian approach to combining animal abundance and demographic data. *Animal Biodiversity and Conservation*, *27*, 515–529.

Burgess, S. C., Baskett, M. L., Grosberg, R. K., Morgan, S. G., & Strathmann, R. R. (2016). When is dispersal for dispersal? Unifying marine and terrestrial perspectives. *Biological Reviews*, *91*, 867–882.

Campbell Grant, E. H., Nichols, J. D., Lowe, W. H., & Fagan, W. F. (2010). Use of multiple dispersal pathways facilitates amphibian persistence in stream networks. *Proceedings of the National Academy of Sciences of the United States of America*, *107*, 6936–6940.

Cavanaugh, K. C., Carroll, D., Bardou, R., & Van der Stocken, T. (2024). Dispersal limits poleward expansion of mangroves on the west coast of North America. *Ecography*, *2024*, e07288.

Clement, M. J., Royle, J. A., & Mixan, R. J. (2022). Estimating occupancy from autonomous recording unit data in the presence of misclassifications and detection heterogeneity. *Methods in Ecology and Evolution*, *13*, 1719–1729.

Clobert, J., Danchin, E., Dhondt, A. A., & Nichols, J. D. (2001). *Dispersal*. Oxford University Press.

Clobert, J., Le Galliard, J. F., Cote, J., Meylan, S., & Massot, M. (2009). Informed dispersal, heterogeneity in animal dispersal syndromes and the dynamics of spatially structured populations. *Ecology Letters*, *12*, 197–209.

Dail, D., & Madsen, L. (2011). Models for estimating abundance from repeated counts of an open metapopulation. *Biometrics*, *67*, 577–587.

De Bona, S., Bruneaux, M., Lee, A. E. G., Reznick, D. N., Bentzen, P., & López-Sepulcre, A. (2019). Spatio-temporal dynamics of density-dependent dispersal during a population colonisation. *Ecology Letters*, *22*, 634–644.

de Valpine, P., Turek, D., Paciorek, C. J., Anderson-Bergman, C., Lang, D. T., & Bodik, R. (2017). Programming with models: Writing statistical algorithms for general model structures with NIMBLE. *Journal of Computational and Graphical Statistics*, *26*, 403–413.

deMaynadier, P., & Houlahan, J. (2007). Conserving vernal Pool amphibians in managed forests. In A. Calhoun & P. G. DeMaynadier (Eds.), *Science and conservation of vernal pools in northeastern North America* (pp. 253–280). CRC Press.

Didan, K. (2021). *MODIS/Terra vegetation indices 16-day L3 global 250 m SIN grid V061 [dataset]*. NASA Land Processes Distributed Active Archive Center.

Doerr, V. A. J., Barrett, T., & Doerr, E. D. (2011). Connectivity, dispersal behaviour and conservation under climate change: A response to Hodgson et al. *Journal of Applied Ecology*, *48*, 143–147.

Esler, D. (2000). Applying metapopulation theory to conservation of migratory birds. *Conservation Biology*, *14*, 366–372.

Fletcher, R. J., Hefley, T. J., Robertson, E. P., Zuckerberg, B., McCleery, R. A., & Dorazio, R. M. (2019). A practical guide for combining data to model species distributions. *Ecology*, *100*, e02710.

Foppen, R. P. B., Chardon, J. P., & Liefveld, W. (2000). Understanding the role of sink patches in source-sink metapopulations: Reed warbler in an agricultural landscape. *Conservation Biology*, *14*, 1881–1892.

Fretwell, S. D., & Lucas, H. L. (1969). On territorial behavior and other factors influencing habitat distribution in birds—I. Theoretical development. *Acta Biotheoretica*, *19*, 16–36.

Fukuda, Y., Moritz, C., Jang, N., Webb, G., Campbell, H., Christian, K., Lindner, G., & Banks, S. (2022). Environmental resistance and habitat quality influence dispersal of the saltwater crocodile. *Molecular Ecology*, *31*, 1076–1092.

Haché, S., Villard, M. A., & Bayne, E. M. (2013). Experimental evidence for an ideal free distribution in a breeding population of a territorial songbird. *Ecology*, *94*, 861–869.

Hanski, I. (1994). A practical model of metapopulation dynamics. *Journal of Animal Ecology*, *63*, 151–162.

Hanski, I. (1998). Metapopulation dynamics. *Nature*, *396*, 41–49.

Haughland, D. L., & Larsen, K. W. (2004). Exploration correlates with settlement: Red squirrel dispersal in contrasting habitats. *Journal of Animal Ecology*, *73*, 1024–1034.

Hebblewhite, M., & Haydon, D. T. (2010). Distinguishing technology from biology: A critical review of the use of GPS telemetry data in ecology. *Philosophical Transactions of the Royal Society, B: Biological Sciences*, *365*, 2303–2312.

Hostetler, J. A., & Chandler, R. B. (2015). Improved state-space models for inference about spatial and temporal variation in abundance from count data. *Ecology*, *96*, 1713–1723.

Howe, R. W., Davis, G. J., & Mosca, V. (1991). The demographic significance of "sink" populations. *Biological Conservation*, *57*, 239–255.

Howell, P. E., Hossack, B. R., Muths, E., Sigafus, B. H., & Chandler, R. B. (2020). Informing amphibian conservation efforts with abundance-based metapopulation models. *Herpetologica*, *76*, 240–250.

Howell, P. E., Muths, E., Hossack, B. R., Sigafus, B. H., & Chandler, R. B. (2018). Increasing connectivity between metapopulation ecology and landscape ecology. *Ecology*, *99*, 1119–1128.

Ims, R. A., & Andreassen, H. P. (2005). Density-dependent dispersal and spatial population dynamics. *Proceedings of the Royal Society B: Biological Sciences*, *272*, 913–918.

Jønsson, K. A., Tøttrup, A. P., Borregaard, M. K., Keith, S. A., Rahbek, C., & Thorup, K. (2016). Tracking animal dispersal: From individual movement to community assembly and global range dynamics. *Trends in Ecology & Evolution*, *31*, 204–214.

Kendall, W. L., & Pollock, K. H. (1992). The robust design in capture-recapture studies: A review and evaluation by Monte Carlo simulation. In D. R. McCullough & R. H. Barrett (Eds.), *Wildlife 2001: Populations* (pp. 31–43). Springer Netherlands.

Kervellec, M., Couturier, T., Bauduin, S., Chenesseau, D., Defos du Rau, P., Drouet-Hoguet, N., Duchamp, C., Steinmetz, J., Vandel, J. M., & Gimenez, O. (2024). Bringing circuit theory into spatial occupancy models to assess landscape connectivity. *Methods in Ecology and Evolution*, *15*, 2141–2152.

Korsten, P., Van Overveld, T., Adriaensen, F., & Matthysen, E. (2013). Genetic integration of local dispersal and exploratory behaviour in a wild bird. *Nature Communications*, *4*, 2362.

Lebreton, J. D., Nichols, J. D., Barker, R. J., Pradel, R., & Spendelow, J. A. (2009). Modeling individual animal histories with multistate capture-recapture models. *Advances in Ecological Research*, *41*, 87–173.

Leirs, H., Stenseth, N. C., Nichols, J. D., Hines, J. E., Verhagen, R., & Verheyen, W. (1997). Stochastic seasonality and nonlinear density-dependent factors regulate population size in an African rodent. *Nature*, *389*, 176–180.

Lin, Y. T. K., & Batzli, G. O. (2001). The influence of habitat quality on dispersal, demography, and population dynamics of voles. *Ecological Monographs*, *71*, 245–275.

Madsen, L., & Royle, J. A. (2023). A review of N-mixture models. *WIREs Computational Statistics*, *15*, e1625.

Matthysen, E. (2005). Density-dependent dispersal in birds and mammals. *Ecography*, *28*, 403–416.

McCrea, R. S., Morgan, B. J. T., Gimenez, O., Besbeas, P., Lebreton, J. D., & Bregnballe, T. (2010). Multi-site integrated population modelling. *Journal of Agricultural, Biological, and Environmental Statistics*, *15*, 539–561.

Miller, D. A. W., Pacifici, K., Sanderlin, J. S., & Reich, B. J. (2019). The recent past and promising future for data integration methods to estimate species' distributions. *Methods in Ecology and Evolution*, *10*, 22–37.

Morris, T. P., White, I. R., & Crowther, M. J. (2019). Using simulation studies to evaluate statistical methods. *Statistics in Medicine*, *38*, 2074–2102.

Ng, W. H., Fink, D., La Sorte, F. A., Auer, T., Hochachka, W. M., Johnston, A., & Dokter, A. M. (2022). Continental-scale biomass redistribution by migratory birds in response to seasonal variation in productivity. *Global Ecology and Biogeography*, *31*, 727–739.

Nichols, J. D., Hines, J. E., Sauer, J. R., Fallon, F. W., Fallon, J. E., & Heglund, P. J. (2000). A double-observer approach for estimating detection probability and abundance from point counts. *Auk*, *117*, 393–408.

Pacifici, K., Reich, B. J., Miller, D. A. W., Gardner, B., Stauffer, G., Singh, S., McKerrow, A., & Collazo, J. A. (2017). Integrating multiple data sources in species distribution modeling: A framework for data fusion. *Ecology*, *98*, 840–850.

Patrick, D. A., Harper, E. B., Hunter, M. L., & Calhoun, A. J. K. (2008). Terrestrial habitat selection and strong density-dependent mortality in recently metamorphosed amphibians. *Ecology*, *89*, 2563–2574.

Pavlacky, D. C., Lukacs, P. M., Blakesley, J. A., Skorkowsky, R. C., Klute, D. S., Hahn, B. A., Dreitz, V. J., George, T. L., & Hanni, D. J. (2017). A statistically rigorous sampling design to integrate avian monitoring and management within bird conservation regions. *PLoS One*, *12*, e0185924.

Peniston, J. H., Backus, G. A., Baskett, M. L., Fletcher, R. J., & Holt, R. D. (2023). Ecological and evolutionary consequences of temporal variation in dispersal. *Ecography*, *2024*, e06699.

Pinto, S. M., & MacDougall, A. S. (2010). Dispersal limitation and environmental structure interact to restrict the occupation of optimal habitat. *American Naturalist*, *175*, 675–686.

Pittman, S. E., Osbourn, M. S., & Semlitsch, R. D. (2014). Movement ecology of amphibians: A missing component for understanding population declines. *Biological Conservation*, *169*, 44–53.

Pollock, K. H. (1982). A capture-recapture design robust to unequal probability of capture. *The Journal of Wildlife Management*, *46*, 752–757.

R Development Core Team. (2019). *R: A language and environment for statistical computing*. R Foundation for Statistical Computing.

Renfrew, R. B., Kim, D., Perlut, N., Smith, J., Fox, J., & Marra, P. P. (2013). Phenological matching across hemispheres in a long-distance migratory bird. *Diversity and Distributions*, *19*, 1008–1019.

Royle, J. A., Dawson, D. K., & Bates, S. (2004). Modeling abundance effects in distance sampling. *Ecology*, *85*, 1951–1957.

Sauer, J. R., Pardieck, K. L., Ziolkowski, D. J., Smith, A. C., Hudson, M. A. R., Rodriguez, V., Berlanga, H., Niven, D. K., & Link, W. A. (2017). The first 50 years of the North American breeding bird survey. *Condor*, *119*, 576–593.

Schaub, M., & Abadi, F. (2011). Integrated population models: A novel analysis framework for deeper insights into population dynamics. *Journal für Ornithologie*, *152*, S227–S237.

Schaub, M., & Kéry, M. (2022). *Integrated population models: Theory and ecological applications with R and JAGS*. Academic Press.

Schwarz, C. J., Schweigert, J. F., & Arnason, A. N. (1993). Estimating migration rates using tag-recovery data. *Biometrics*, *49*, 177–193.

Serrano, D., & Tella, J. L. (2003). Dispersal within a spatially structured population of lesser kestrels: The role of spatial isolation and conspecific attraction. *Journal of Animal Ecology*, *72*, 400–410.

Shurin, J. B., Cottenie, K., & Hillebrand, H. (2009). Spatial autocorrelation and dispersal limitation in freshwater organisms. *Oecologia*, *159*, 151–159.

Stevens, D. L., & Olsen, A. R. (2004). Spatially balanced sampling of natural resources. *Journal of the American Statistical Association*, *99*, 262–278.

Swift, R. J., Anteau, M. J., Ellis, K. S., MacDonald, G. J., Ring, M. M., Sherfy, M. H., Toy, D. L., & Koons, D. N. (2025). Not all spatially structured populations are metapopulations: Re-examining paradigms for a threatened shorebird. *Ecological Applications*, *35*, e70037.

Szulkin, M., & Sheldon, B. C. (2008). Dispersal as a means of inbreeding avoidance in a wild bird population. *Proceedings of the Royal Society B: Biological Sciences*, *275*, 703–711.

Turek, D., de Valpine, P., & Paciorek, C. J. (2025). nimbleHMC: Hamiltonian Monte Carlo and Other gradient-based MCMC sampling algorithms for "nimble". *The Journal of Open Source Software*, *9*, 6745.

van der Hammen, T., Montserrat, M., Sabelis, M. W., de Roos, A. M., & Janssen, A. (2012). Whether ideal free or not, predatory mites distribute so as to maximize reproduction. *Oecologia*, *169*, 95–104.

Van Ee, J. J., Hagen, C. A., Pavlacky, D. C., Jr., Haukos, D. A., Lawrence, A. J., Tanner, A. M., Grisham, B. A., Fricke, K. A., Rossi, L. G., Beauprez, G. M., Kuklinski, K. E., Martin, R. L., Koslovsky, M. D., Rintz, T. B., & Hooten, M. B. (2024). Melded integrated population models. *Journal of Agricultural, Biological, and Environmental Statistics*, *1*, 1–31.

Walhström, L. K., & Kjellander, P. (1995). Ideal free distribution and natal dispersal in female roe deer. *Oecologia*, *103*, 302–308.

Wells, K. D. (1977). The social behaviour of anuran amphibians. *Animal Behaviour*, *25*, 666–693.

Wolff, J. O., Lundy, K. I., & Baccus, R. (1988). Dispersal, inbreeding avoidance and reproductive success in white-footed mice. *Animal Behaviour*, *36*, 456–465.

Zammarelli, M. B., Ayres, M. P., Ter Hofstede, H. M., Lutz, D. A., & Holmes, R. T. (2024). Territory sizes and patterns of habitat use by forest birds over five decades: Ideal free or ideal despotic? *Ecology Letters*, *27*, e14525.

Zhao, Q. (2020). On the sampling design of spatially explicit integrated population models. *Methods in Ecology and Evolution*, *11*, 1207–1220.

Zhao, Q. (2024). *Bayesian analysis of spatially structured population dynamics*. Springer.

Zhao, Q. (2026). Code and data for "spatially realistic dynamic N-mixture models". *Zenodo*. https://doi.org/10.5281/zenodo.21535376

Zhao, Q., Fuller, A. K., & Royle, J. A. (2022). Spatial dynamic N-mixture models with interspecific interactions. *Methods in Ecology and Evolution*, *13*, 2209–2221.

Zhao, Q., Latif, Q. S., Nuse, B. L., Pavlacky, D. C., Kilner, C. L., Ryder, T. B., & Latimer, C. E. (2024). Integrating counts from rigorous surveys and participatory science to better understand spatiotemporal variation in population processes. *Methods in Ecology and Evolution*, *15*, 1380–1393.

Zhao, Q., & Royle, J. A. (2019). Dynamic N-mixture models with temporal variability in detection probability. *Ecological Modelling*, *393*, 20–24.

Zhao, Q., Royle, J. A., & Boomer, G. S. (2017). Spatially explicit dynamic N-mixture models. *Population Ecology*, *59*, 293–300.

How to cite this article: Zhao, Q., Howell, P. E., Muths, E., Sigafus, B. H., Hossack, B. R., & Latimer, C. E. (2026). Spatially realistic dynamic N-mixture models. *Methods in Ecology and Evolution*, *00*, 1–16. https://doi.org/10.1111/2041-210x.70389